

Fast Colon Centreline Calculation using Optimised 3D

Topological Thinning

Robert J.T. Sadleir and Paul F. Whelan

Vision Systems Group, Dublin City University, Ireland.

Name and address for correspondence:

Robert J.T. Sadleir,

Vision Systems Group,

School of Electronic Engineering,

Dublin City University,

Dublin 9,

Ireland.

Tel: +353 1 7008592

Fax: +353 1 7005508

E-mail: Robert.Sadleir@dcu.ie

ABSTRACT

Topological thinning can be used to accurately identify the central path through a computer model of the colon generated using computed tomography colonography. The central path can subsequently be used to simplify the task of navigation within the colon model. Unfortunately standard topological thinning is an extremely inefficient process. We present an optimised version of topological thinning that significantly improves the performance of centreline calculation without compromising the accuracy of the result.

Keywords:

Colon, Computed Tomography Colonography, Centreline, 3D Topological Thinning, Virtual Endoscopy.

1. INTRODUCTION

Virtual reality imaging of the colon using computed tomography (CT) data was originally demonstrated by Vining et al. (1) in 1994. This technique, more recently known as CT Colonography (CTC) (2), is a minimally invasive alternative to conventional colonoscopy for colon imaging. CTC involves generating a computer model of the colon using data obtained from an abdominal CT study of a suitably prepared patient. The resulting virtual colon can be examined in a manner similar to conventional colonoscopy.

Unaided endoluminal navigation at CTC is impractical due in part to the tortuous nature of the colon. This problem can be alleviated to some extent by identifying an approximation of the central path through the colon. This path is commonly referred to as the colon centreline. The centreline can subsequently be used to constrain and thus greatly simplify the task of endoluminal navigation.

Identifying the centreline of the colon at CTC is not a trivial process. This task is compounded by the sheer volume of data contained in a CTC dataset in addition to the complicated morphology of the colon. Ideally, a centreline calculation algorithm should generate an accurate approximation of the central path through the colon with minimal operator intervention in a reasonable amount of time. The time constraint is especially important considering the potential deployment of such an algorithm in a clinical environment. The problem of centreline calculation has received a great deal of attention since the introduction of CTC and a vast number of centreline calculation algorithms have been described in the literature. These algorithms are briefly summarised and compared (where possible) in Tab. 1.

A number of early centreline calculation algorithms (18, 19) were based on a technique known as onion peeling or topological thinning (20). The use of standard topological thinning for this type of application is considered by many to produce accurate results (3, 8, 10, 11, 15) however it is also regarded as being extremely inefficient (3, 7, 8, 11, 12, 14, 15). As a result the majority of recently published approaches either describe efficient alternatives to topological thinning or modifications to the standard topological thinning algorithm that increase performance.

Ge et al. (13) provide an excellent example of a centreline calculation algorithm based on topological thinning (summarised in Fig. 1). Their multistage algorithm begins by identifying voxels that represent the colon lumen. This process, known as segmentation, is achieved using a simple 3D region growing algorithm. A topological thinning algorithm is subsequently employed to obtain a skeleton representation of the segmented colon lumen. Finally, the centreline is obtained by reducing the skeleton to a single centred path between two user defined endpoints. Optimisation techniques including surface voxel tracking and dataset subsampling are employed to improve performance. Centreline calculation using this approach requires approximately 60 seconds. Although this is relatively fast it is still significantly slower than more recent alternatives.

In this article we describe a fast colon centreline calculation algorithm using an optimised approach to 3D topological thinning. We begin by summarising a standard approach to centreline calculation using topological thinning that is loosely based on

the technique described by Ge et al. (13). Then we outline how the performance of this approach can be significantly improved by employing a lookup-table (LUT) based optimisation technique. Finally we present the results of our study comparing the performance of these two techniques and comment on the significance of these results before concluding the article.

2. METHODS

2.1 Patient preparation and data acquisition

Prior to their scheduled examination all patients were instructed to take a low-residue diet for 48 hours followed by clear fluids for 24 hours. Prior to the day of examination, patients were instructed to take one sachet of Pixcolax at 08.00, a second sachet of Pixcolax at 12.00, a sachet of clean prep in a litre of cold water at 18.00 and a Senokot tablet at 23.00. Immediately before the examination the colon was gently insufflated with room air to the maximum tolerable level and the patient was subsequently scanned in both the supine and prone positions to reduce the effect of residual material in the colon.

All scans were obtained using a Siemens Somatom 4, four slice multidetector Spiral CT scanner. The scanning parameters were 120kVp, 2.5mm collimation, 3mm slice thickness, 1.5mm reconstruction interval, 0.6s gantry rotation and field of view of 380°. The scanning time ranges from 20-30s, so the acquisition is performed in single breath-hold. The procedure was first performed with the patient in the supine position and then repeated with the patient in the prone position. The number of slice varies from approximately 250-300 depending on the height of the patient and each slice

comprised of approximately 512 x 512 pixels. Typical total size of the volumetric data is approximately 150Mbytes

2.2 Segmentation and endpoint detection

The colon lumen is extracted from the CTC dataset using a standard region growing based segmentation technique (21, 22). Segmentation results in a binary model of the colon lumen consisting of only object [1] and background [0] voxels. The two endpoints required for centreline calculation can be automatically identified during the segmentation process using a technique based on distance fields (8). Any cavities, i.e. background voxels located within the segmented colon lumen, may adversely affect skeleton generation and must be removed. Finally, the volume is cropped to the minimum size required to enclose the entire segmented colon lumen. The resulting solid binary object and endpoint pair constitute the inputs to the centreline calculation algorithm

2.3. Skeleton generation

The skeleton of the segmented colon lumen is obtained using topological thinning. The thinning process involves the removal of layers of surface voxels from a binary object. A surface voxel, i.e. one that is not completely surrounded by other object voxels, is only removed if it does not affect certain structural properties of the object being thinned. These properties describe the object in terms of overall connectivity, holes and endpoints. Layers of surface voxels are removed iteratively and the process terminates when no more surface voxels can be removed without compromising the structural properties outlined above. The resulting set of voxels represents the skeleton of the original object.

The initial set of surface voxels are identified by performing a raster scan of the entire volume. Subsequent surface voxels can be identified more easily by examining the 6 directly connected neighbours of deleted voxels. A total of three tests must be performed prior to the deletion of a particular surface voxel, these tests deal with the following requirements:

1. **Endpoint retention:** The number and location of endpoints in the skeleton must be the same as in the original object. In the case of centreline calculation there are only two endpoints of interest, these are located in the rectum and caecum.
2. **Connectivity preservation:** The number of distinct binary objects in the scene must be the same before and after the application of the topological thinning algorithm.
3. **Hole prevention:** The removal of a surface voxel must not introduce a new hole into the object being thinned.

If the deletion of a particular surface voxel respects all of these requirements then it is removed otherwise it is retained possibly to be deleted at a subsequent iteration. The endpoint retention test is trivial and involves comparing the coordinates of the voxel under examination with those of the two predefined endpoints. The other two tests, connectivity preservation and hole prevention, are much more complicated and require a significant amount time to perform. In each of these cases the test involves extensively examining the configuration of the 26 voxels in the $3 \times 3 \times 3$ region surrounding the deletion candidate.

2.4. Skeleton reduction (centreline generation)

The skeleton that results from the topological thinning stage incorporates the colon centreline. Unfortunately, it also includes a number of extraneous loops that occur due to holes in the original segmented colon lumen (see Fig. 2a). These holes are a common occurrence usually associated with the Haustral folds. The skeleton branches caused by holes are closer to the surface of the colon than those associated with the actual centreline. The proximity of a particular skeleton voxel to the original surface is related to the thinning iteration at which that voxel was uncovered. By assigning the relevant thinning index to each voxel as it is exposed it is possible to generate a distance field that represents the approximate distance of each lumen voxel from the colon surface. Following an inversion of the distance values it is possible to generate a weighted graph where the centreline can be identified as the minimum cost path between the two predefined endpoints. The minimum cost path can be found in an extremely efficient manner using a simplified version of the Dijkstra shortest path algorithm (23). The resulting set of points represents the final centreline, i.e. the path between the two predefined endpoints that is furthest from the surface of the original segmented colon lumen (see Fig. 2b). The skeleton reduction process is illustrated in Fig. 3 using a 2D example.

2.5. Optimisation

The method for centreline calculation outlined in the previous paragraphs forms the basis for our optimised implementation and will be used as a standard for comparison purposes. Our enhancements deal specifically with the skeleton generation stage, particularly the tests for connectivity preservation and hole prevention. Both of these tests must be performed repeatedly, at least once for each object voxel, and represent the most time consuming aspect of the centreline calculation process. In each case the

3×3×3 neighbourhood surrounding the voxel under examination is extensively analysed in order establish whether its removal will affect the relevant global properties of the object, i.e. overall connectivity and number of holes. The result of this analysis is dependant on the values of the 26 neighbours surrounding the voxel under examination. Each of these voxels can belong to one of two classes, either object or background, consequently the number of possible neighbourhood configurations is 67,108,864 (2^{26}).

In order to streamline the centreline calculation process we generate all possible neighbourhood configurations. Each neighbourhood is tested for connectivity preservation and hole prevention. The results of these tests are combined into a single pass/fail binary value and stored in a LUT structure. Each result is addressed by a unique index, I , that is obtained by multiplying the value of each voxel in the neighbourhood ($V_0 - V_{25}$) with a weight in the range $2^0 - 2^{25}$ and then summing the results:

$$I = \sum_{n=0}^{25} 2^n V_n \quad (1)$$

This is essentially a 3D convolution operation where the value of the central voxel is not used in the calculation. A simplified 2D example of the index generation process is illustrated in Fig. 4.

The LUT can subsequently be used to streamline the standard centreline calculation algorithm. During the thinning phase of the algorithm, the computationally intensive tests for connectivity preservation and hole prevention are no longer necessary. Instead, the relevant index is quickly generated using the equation above and the LUT is queried to determine whether or not the central voxel can be removed. The thinning

process continues until only skeleton voxels remain and the skeleton is reduced using the technique described earlier to obtain the final centreline.

It is extremely important to note that the LUT is calculated only once. It is subsequently stored in a file on the hard disk and reloaded (not recalculated) each time it is required for centreline calculation. The time required to load the LUT is significantly less than the time required to generate it.

3. RESULTS

We evaluated both the standard and optimised centreline calculation algorithms using 12 CTC datasets (6 prone and 6 supine) that were acquired from our CTC database. Only datasets with intact colons, i.e. colons without collapse or extreme blockage, were selected. Examples of the centreline obtained are illustrated in Fig 5. Both techniques produced perfectly matching centrelines in all cases. The comparison was performed by calculating the distance from each voxel in the optimised centreline with the nearest pixel in the standard centreline. In all cases the sum of these distances was zero. The average time required for centreline calculation using the standard approach was 155.413 seconds compared to 3.438 seconds for the optimised approach (see Table 2 for a detailed breakdown of results). The once off task of lookup table initialisation required approximately 1.5 hours. However, loading the table prior to each centreline calculation required less than 1 second. All software was implemented using the Java 2 standard edition version 1.4.2 (Sun Microsystems Inc., Santa Clara, CA, USA) and tested on a standard PC workstation (1.6 GHz CPU and 512 Mb RAM) running Microsoft Windows XP professional (Microsoft Corp., Redmond, WA, USA). Note that similar results were obtained using a C++ implementation of

our optimised centreline calculation algorithm running on the same hardware platform.

4. DISCUSSION

Centreline calculation using standard topological thinning is an extremely time consuming process. We have described how the performance of topological thinning can be improved by utilising a LUT to significantly reduce demand on the CPU. We have demonstrated how our optimised approach outperforms standard topological thinning based centreline calculation with execution times that are an average of 45 times faster than the standard approach. Our modifications are relatively straightforward to implement and do not alter the core functionality of the topological thinning algorithm, hence the quality of the resulting centreline is not compromised. The only time consuming aspect of our approach is the task of lookup table population. This requires extensively analysing over 67 million neighbourhoods and requires several hours to complete. Fortunately once generated the same lookup table can be used for all subsequent centreline calculations.

The centreline calculation technique described in this paper deals with intact colons, i.e. colons where there is an unobstructed path between the rectum and the caecum. Consequently this technique is not restricted to applications in CTC and can be used in other areas of virtual endoscopy where a single path or even multiple flight paths are required for a hollow object. In the case of colons with collapsed segments or extreme blockages, segmentation of the colon will yield a number of subsections that represent the air filled colon lumen. Here the centreline calculation algorithm must be applied to each of the individual sections and the centreline segments can then be

combined to yield the final result. Dealing with the problem of collapsed and blocked colons falls into the realm of segmentation and a method developed by our group for automatic segmentation of collapsed and blocked colons is the subject of another paper (currently under review elsewhere – reference provided when available). Fig 6 provides some examples of how our centreline calculation algorithm can be used in cases where colon segmentation yields multiple segments.

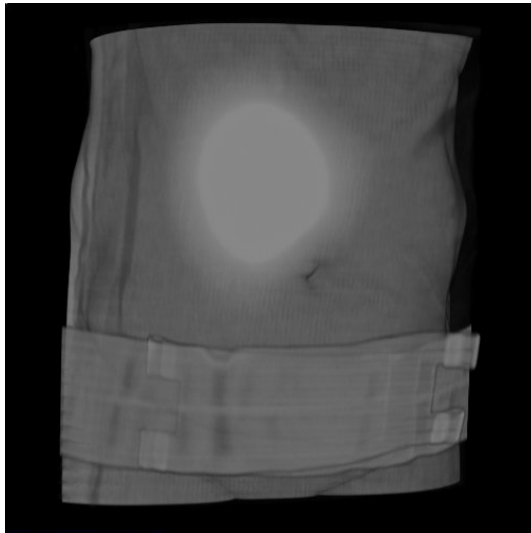
REFERENCES

1. Vining DJ, Gelfand, DW, Bechtold, RE, Scharling, ES.; Grishaw, EK. and Shifrin, RY. Technical feasibility of colon imaging with helical CT and virtual reality. *AJR*. 1994;162(S):104.
2. Johnson CD, Hara AK, Reed JE. Virtual endoscopy: what's in a name? *AJR* 1998;171(5):1201-2.
3. Wan M, Liang Z, Ke Q, Hong L, Bitter I and Kaufman A. Automatic centerline extraction for virtual colonoscopy. *IEEE Trans Med Imaging* 2002; 21(12):1450-60.
4. Sadleir RJT, Whelan PF. Colon centreline calculation for CT colonography using optimised 3D topological thinning. *Proc. First International Symposium on 3D Data Processing, Visualization and Transmission* 2002:800-3.
5. Deschamps T, Cohen LD. Fast extraction of minimal paths in 3D images and applications to virtual endoscopy. *Med Image Anal* 2001;5(4):281-99.
6. Chen D, Li B, Liang Z, Wan M, Kaufman AE and Wax M. Tree-branch searching multiresolution approach to skeletonization for virtual endoscopy. *Proc. SPIE Medical Imaging: Image Processing* 2000;3979:726-34.

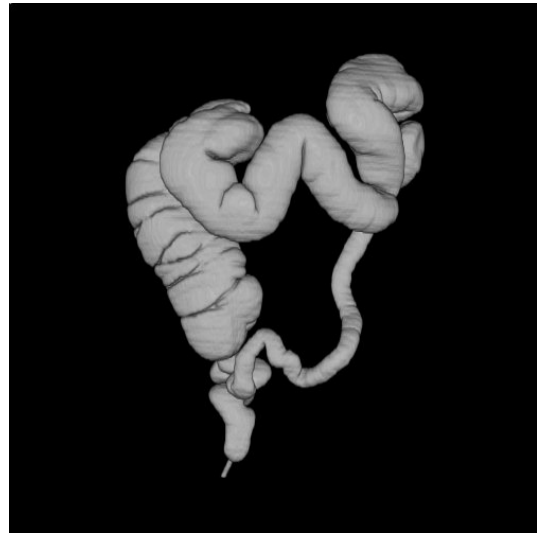
7. Samara Y, Fiebich M, Dachman AH, Doi K and Hoffmann KR. Automated centreline tracking of the human colon. Proc. SPIE Medical Imaging: Image Processing 1998;3338:740-6.
8. Bitter I, Kaufman AE, Sato M. Penalized-distance volumetric skeleton algorithm. IEEE Trans Vis Comp Graph 2001;7(3):195-206.
9. Zhou Y, Kaufman A, Toga AW. Three-dimensional skeleton and centerline generation based on an approximate minimum distance field. Visual Comput 1998;14(7):303-14.
10. Sato M, Bitter I, Bender M, Kaufman A and Nakajima M. TEASAR: Tree-structure extraction algorithm for accurate and robust skeletons. Proc. Pacific Graphics 2000:281-9.
11. Bitter I, Sato M, Bender M, McDonnell KT, Kaufman A and Wan M. CEASAR: A smooth, accurate and robust centreline extraction algorithm. Proc. IEEE Visualisation 2000:45-52.
12. Samara Y, Fiebich M, Dachman AH, Kuniyoshi JK, Doi K and Hoffmann KR. Automated calculation of the centerline of the human colon on CT images. Acad Radiol 1999;6(6):352-9.
13. Ge Y, Stelts DR, Wang J, Vining DJ. Computing the centerline of a colon: a robust and efficient method based on 3D skeletons. J Comput Assist Tomogr 1999;23(5):786-94.
14. Zhou Y, Toga AW. Efficient skeletonization of volumetric objects. IEEE Trans Vis Comp Graph 1999;5(3):196-209.
15. Paik DS, Beaulieu CF, Jeffrey RB, Rubin GD and Napel S. Automated flight path planning for virtual endoscopy. Med Phys 1998;25(5):629-37.

16. McFarland EG, Wang G, Brink JA, Balfe DM, Heiken JP and Vannier MW. Spiral computer tomographic colonography: determination of the central axis and digital unravelling of the colon. *Acad Radiol* 1997;4(5):367-73.
17. Chiou RCH, Kaufman AE, Liang ZR, Hong LC, and Achiotou M. An interactive fly-path planning using potential fields and cell decomposition for virtual endoscopy. *IEEE Trans Nuc Sci* 1999;46(4):1045-9.
18. Hong L, Kaufman A, Wei YC, Viswambharan, Wax M, Liang Z, Loew M and Gershon N. 3D virtual colonoscopy. *Proc. IEEE Biomedical Visualisation Symposium* 1995:26-32.
19. Ge Y, Stelts DR, Wang J, and Vining DJ. Computing the central path of the colon from CT images. *Proc. SPIE Medical Imaging: Image Processing* 1998;3338:702-13.
20. Tsao YF, Fu KS. A parallel thinning algorithm for 3-D pictures. *Comput Graph Image Proc* 1981;17:315-31.
21. Sato M, Lakare S, Wan M, Kaufman A and Wax M. An automatic colon segmentation for 3D virtual colonoscopy. *IECE Trans Inf Syst* 2000;E84(1):201-8.
22. Wyatt CL, Ge Y, Vining DJ. Automatic segmentation of the colon for virtual colonoscopy. *Comput Med Imaging Graph* 2000;24(1):1-9.
23. Dijkstra EW. A note on two problems in connexion with graphs. *Numer Math* 1959;1:269-71.

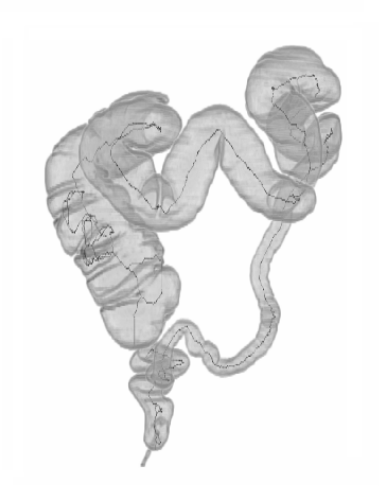
FIGURES



(a)



(b)



(c)



(d)

Fig. 1. An overview of the centreline calculation process. (a) The original CTC dataset; (b) The segmented colon lumen; (c) The skeleton; (d) The final colon centreline.

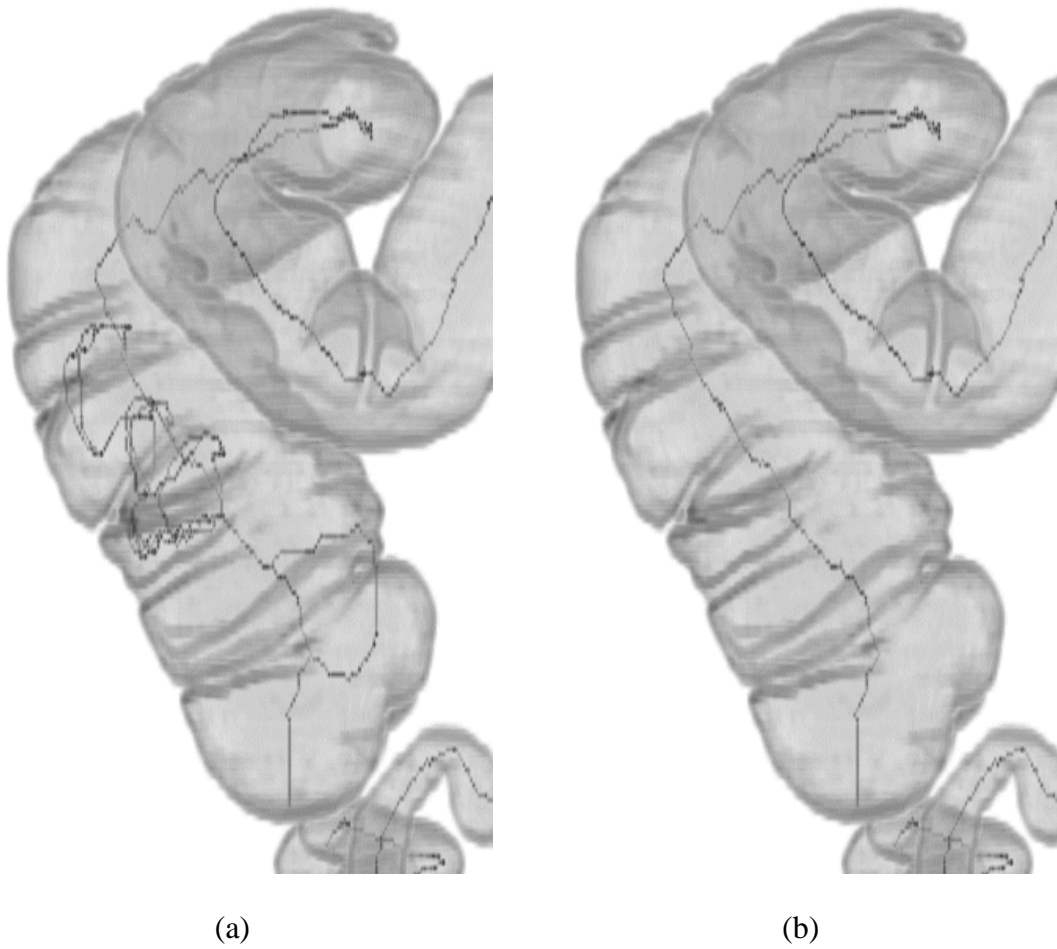


Fig. 2. Magnified sections of the colon lumen from Fig. 1 illustrating how extraneous loops can be caused by the Haustral fold (a) and how the removal of these loops yields the final centreline (b).

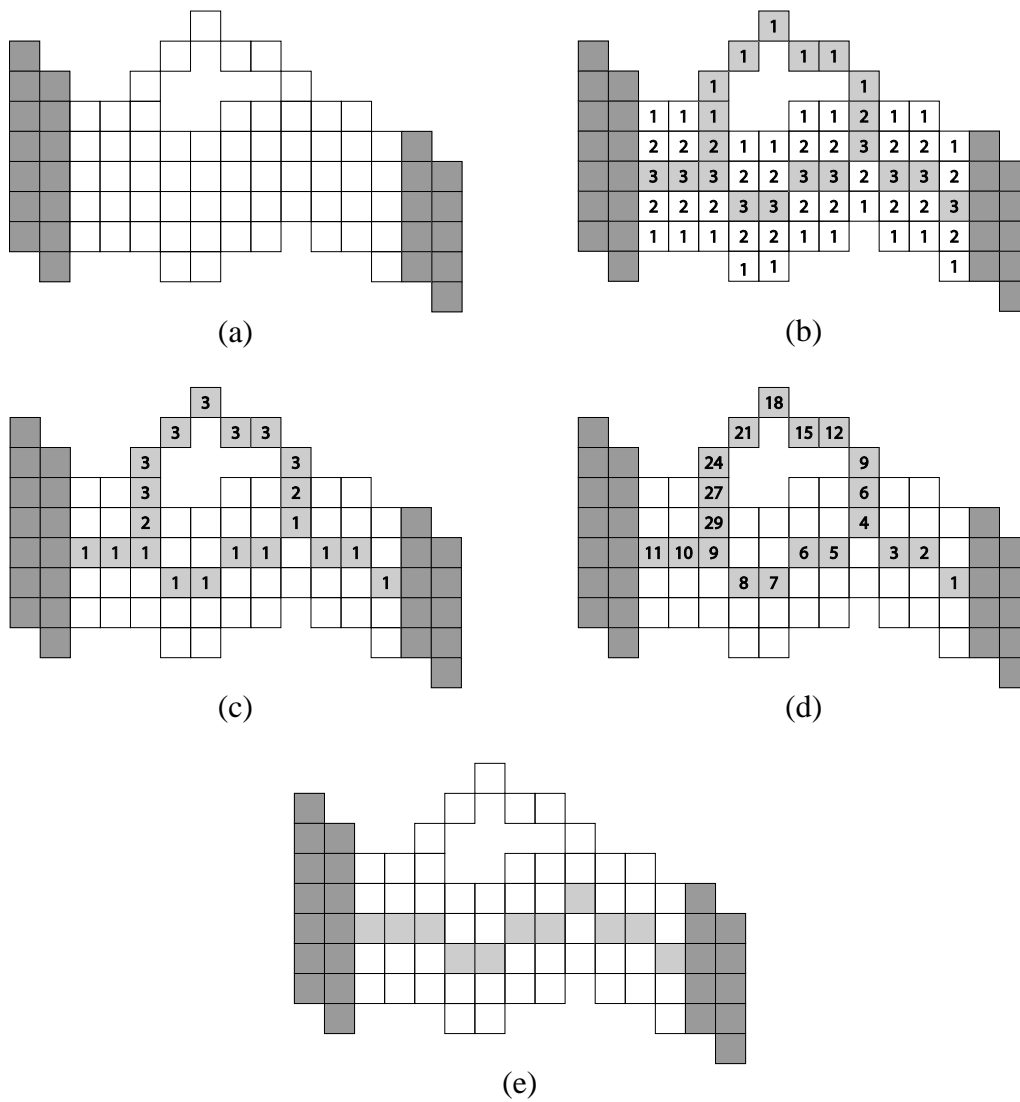


Fig. 3. A 2D example illustrating the skeleton reduction process. (a) Original binary object (region of interest indicated using white); (b) Skeleton and distance from surface field generation; (c) Inverted distance from surface field (skeleton pixels only); (d) weighted graph (originating from the right); (e) The minimum cost path found using backward propagation through the distance field.

General Case:

P_0	P_1	P_2
P_7	x	P_3
P_6	P_5	P_4

 *

2^0	2^1	2^2
2^7	0	2^3
2^6	2^5	2^4

 = LUT Index

Example:

0	0	0
1	x	1
1	1	1

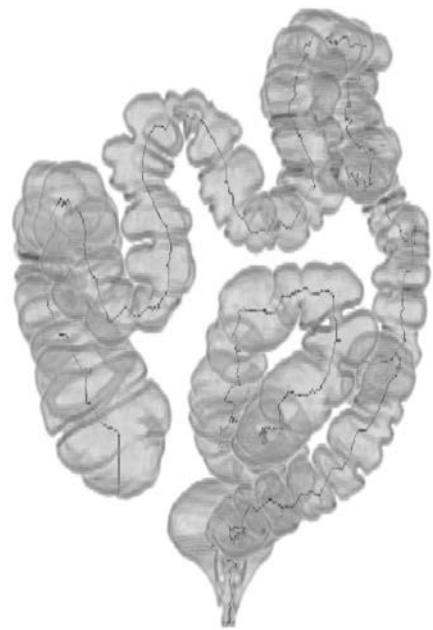
 *

2^0	2^1	2^2
2^7	0	2^3
2^6	2^5	2^4

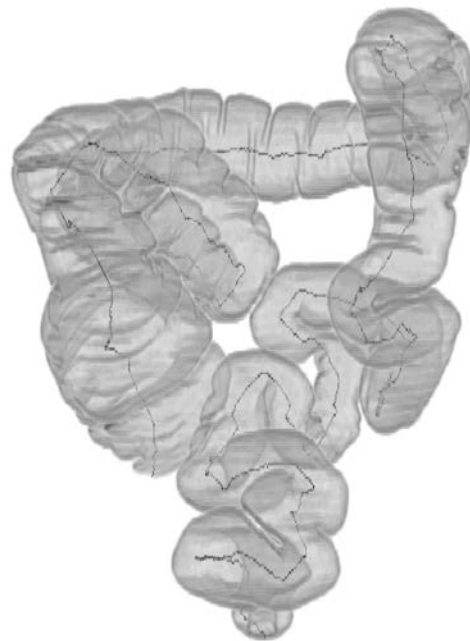
 = 248
(8 + 16 + 32 + 64 + 128)

- 1 Foreground Pixel
- 0 Background Pixel
- x Central Pixel (value irrelevant)
- * Convolution Operation

Fig. 4. A 2D illustration of the LUT index generation process.



(a)



(b)

Fig. 5. Examples of centreline calculation where segmented yielded a single hollow tube connecting the rectum to the caecum.

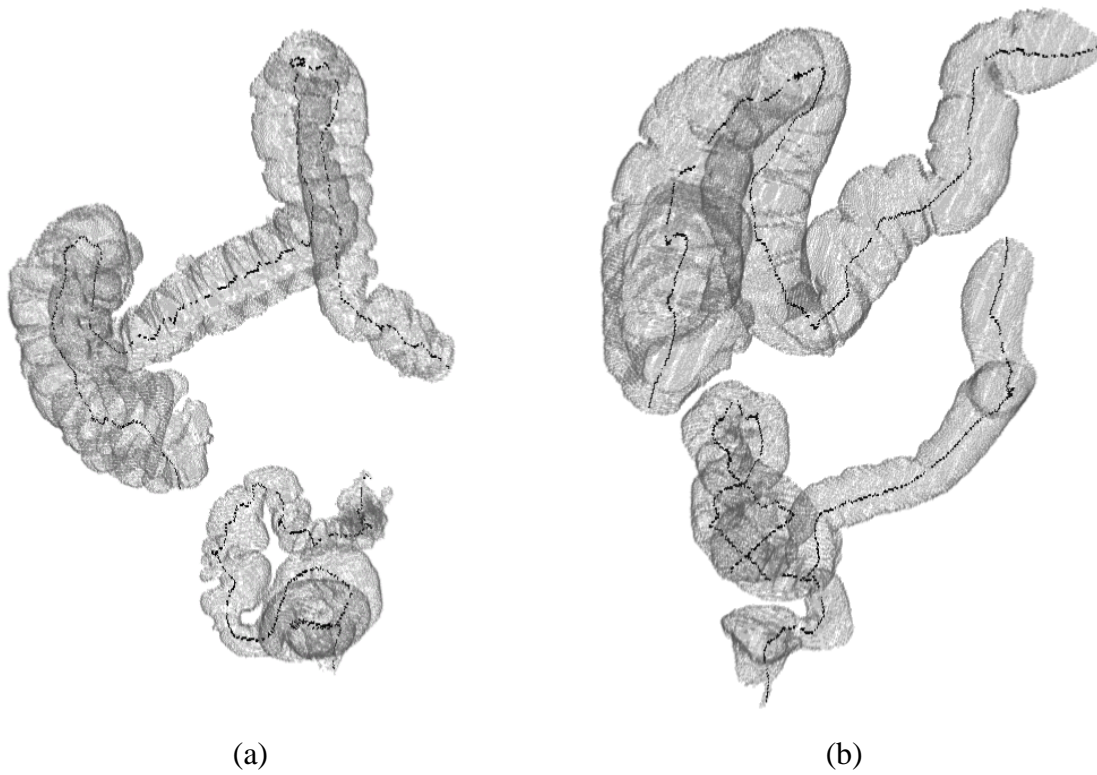


Fig 6. Examples of centreline calculation where the colon is represented by multiple segments (a) blockage in the descending colon and (b) blockage at the splenic flexure.

TABLES

Group	Year	Technique	Platform	CPU (Mhz)	RAM (Mb)	Time (s)
Wan et al. (3)	2002	Minimum cost path through a distance from surface field	Intel	700	655	14.75 ^a
Sadleir and Whelan (4)	2002	Optimized 3D topological thinning using Lookup tables	Intel	700	512	24.42
Deschamps et al. (5)	2001	Minimum energy path through a distance from source field with a centering potential derived from a distance from surface field	Sun/Solaris	300	1024	30
Chen et al (6)	2000	Minimal cost path through a distance from source field followed by a centering stage	SGI	195 x 2 (R10000)	896	36
Samara et al. (7)	1998	Distance from source field with cluster centering	SGI	NA	NA	~60
Bitter et al. (8)	2001	Centerline calculated as minimum cost path from end to start point in a penalized distance field	Intel/Windows	1000	NA	119
Zhou et al (9)	1998	Skeleton extraction using a distance form surface field followed by centerline identification	SGI	NA	NA	199
Sato et al (10)	2000	Centerline calculated as minimum cost path from end to start point in a penalized distance field	SGI	194 (R10000)	NA	208
Bitter et al (11)	2000	Centerline calculated as minimum cost path from end to start point in a penalized distance field	SGI	194 (R10000)	4096	276
Samara et al. (12)	1999	Distance from source field with cluster centering and centerline refinement stage	SGI		896	~300
Ge et al. (13)	1999	3D topological thinning used in conjunction with surface voxel tracking	SGI	NA	NA	518 (60 ^b)
Zhou and Toga (14)	1999	Distance from source field with cluster centers used as centerline points	SGI	NA (R10000)	NA	519
Paik et al. (15)	1998	A combination of a distance from source field and streamlined 3D topological thinning	SGI	180 (R5000)	256	759 ^c
McFarland et al. (16)	1997	Radiologist marking & spline interpolation	NA	NA	NA	1080
Chiou et al. (17)	1999	Identify and connect principle attractors, i.e. local maxima in distance from surface field	SGI	NA	3072	Exact figure unavailable

^adoes not include the time required to generate the distance fields (average time of presented results)

^bobtained by sub sampling the dataset

^cincludes time required for segmentation stage

TABLE 1. A overview of previously published centreline calculation algorithms.

	Dataset A (Best Case)	Dataset B (Worst Case)	Average (all 12 datasets)
Patient position	prone	supine	--
Dataset size (slices)	253	257	272
Lumen size (voxels)	2027478	3473202	2106836
Ratio of centreline/skeleton voxels	0.536	0.398	0.617
Loading LUT (s)	0.844	0.86	0.834
Loading cropped dataset (s)	0.844	1.859	1.409
Surface detection (s)	0.187	0.359	0.279
Skeleton generation (s)	0.734	1.563	0.844
Skeleton reduction (s)	0.141	0.047	0.066
Overall with optimisation t_1 (s)	2.75	4.688	3.438
Overall with out optimisation t_2 (s)	147.453	256.015	155.413
Improvement (t_2 / t_1)	53.619	54.611	44.995

TABLE 2. Detailed results comparing the standard and optimised approaches to centreline calculation. **Note:** our optimisation technique only affected the skeleton generation stage of the centreline calculation process. The time required for all other stages remained the same as the unoptimised approach.